Dynamics and Statistics of Inverse Cascade Processes in 2D Magnetohydrodynamic Turbulence

D. Biskamp and U. Bremer

Max-Planck-Institut für Plasmaphysik, 85748 Garching, Germany

(Received 6 October 1993)

The inverse cascade of the mean square potential A in a 2D magnetofluid randomly forced at small scales is studied by numerical simulations. One finds the spectrum $A_k \simeq 2.6\epsilon_A^{2/3}k^{-7/3}$. The cascade proceeds by coalescence of current filaments, which is a fast reconnection process owing to high turbulent resistivity. Statistics of δv_l and δB_l are strictly Gaussian, also in the condensation phase of A_k at $k = 1$. Only when the coherent magnetic field intensity exceeds that of the fluctuations, non-Gaussian statistics in δB_l occur, which are, however, entirely due to the static magnetic structure and not associated with intermittency of the small-scale turbulence, the latter remaining Gaussian.

PACS numbers: 47.27.Eq, 47.27.Gs, 47.65.+a

Two-dimensional (2D) magnetohydrodynamics (MHD) turbulence has recently attracted considerable interest (see, e.g., [1–4]). Contrary to 2D Navier-Stokes turbulence, which is fundamentally different from that in 3D, 2D and 3D MHD turbulence have many features in common. In particular both exhibit a direct spectral cascade of the energy $E = E^V + E^M = \frac{1}{2}\int(v^2 + B^2)d\tau$ and an inverse cascade of a pure magnetic quantity, the magnetic helicity $H = \frac{1}{2}\int \mathbf{A}\cdot\mathbf{B}\, d\tau$ in 3D and the mean square magnetic potential $A = \frac{1}{2}\int a^2\, d\tau$ in 2D, where a is the component of the vector potential in the third direction. It is generally believed that inverse cascades are the origin of self-organization, i.e., formation of large-scale coherent structures, for instance the isolated vorticity eddies observed in decaying 2D Navier-Stokes turbulence result from the inverse energy cascade [5]. The latter has recently been studied [6], showing that contrary to the behavior in the direct cascade the statistics of the velocity field increments are Gaussian at all scales. Only after the self-similarity of the inverse cascade process is broken due to condensation in the largest possible wavelength non-Gaussian statistics are generated which are attributed to a revival of intermittency of the small-scale turbulence. The question arises whether this behavior is a special property of the 2D Navier-Stokes system, which obeys a particularly simple equation, or is a more generally valid feature of inversely cascading systems. We therefore consider the inverse cascade of A in 2D MHD, which is a more complex system than 2D Navier-Stokes but still allows numerical simulations with high spatial resolution.

When turbulence is excited by injecting A with the rate ϵ_A into some wave-number range around $k \simeq k_0$, the spectral properties for $k < k_0$ are determined by the inverse cascade of A_k. A simple Kolomogorov-type dimensional analysis yields (see, e.g., [1])

$$A_k = C_A\epsilon_A^{2/3}k^{-7/3}, \tag{1}$$

where C_A is a (possibly not universal) constant. The spectrum (1) corresponds to an almost flat magnetic energy spectrum, $E_k^M = k^2A_k \propto k^{-1/3}$. The kinetic energy spectrum E_k^V cannot be determined in this way. The usual way relating E_k^V and E_k^M in the direct energy cascade is provided by the Alfvén effect [7], that due to the influence of the large-scale magnetic field small-scale fluctuations $\tilde{\mathbf{v}}, \tilde{\mathbf{B}}$ are tightly coupled forming Alfvén waves such that $E_k^M \simeq E_k^V$. The Alfvén effect is, however, expected to be weak in the inverse cascade process because of the absence of a significant large-scale field. Direct numerical simulations of the inverse cascade in 2D MHD turbulence have previously been performed [8]; however, the resolution (up to 64^2 collocation points) used was too small to identify an inertial range, and the statistical properties were not addressed. In this Letter we present a series of simulations of rather high resolution (up to 1024^2). The main points investigated are the spectral behavior in the inertial range of the inverse cascade, the dynamics of the cascade process, and the statistical properties in the self-similar cascade and the condensation phases.

The 2D incompressible MHD equations are conveniently written in terms of a and the stream function ϕ assuming uniform mass density $\rho = 1$:

$$\partial_t a + \mathbf{v}\cdot\nabla a = D_a + f_a, \tag{2}$$

$$\partial_t \omega + \mathbf{v}\cdot\nabla\omega - \mathbf{B}\cdot\nabla j = D_\omega + f_\omega, \tag{3}$$

where the magnetic field is $\mathbf{B} = \nabla a \times \hat{\mathbf{z}}$, the velocity $\mathbf{v} = \nabla\phi \times \hat{\mathbf{z}}$, the current density $j = -\nabla^2 a$, and the vorticity $\omega = -\nabla^2\phi$. D_a and D_ω are the magnetic and kinetic dissipation terms. In order to concentrate dissipation at small scales we use higher order diffusion operators, $D_a = -\eta_4\triangle^{(4)}a$, $D_\omega = -\nu_4\triangle^{(4)}\omega$, which have been found in studies of decaying turbulence [3] to allow efficient energy absorption without perturbing the inertial range properties. The external forces f_a, f_ω are applied in a narrow wave-number band Δk around k_0, where $k_0 = 100$ for 512^2 resolution and $k_0 = 250$ for 1024^2 resolution, $\Delta k = 5$, and $\eta_4 = \nu_4$ is chosen such that the residual dissipation for $k < k_0$ is very small. In most cases reported here we choose white-noise Gaussian random forces. The

0031-9007/94/72(24)/3819(4)$06.00

A_k cascade is most clearly observed when the system is driven only magnetically, $f_\omega = 0$, to which case consideration is restricted here. Equations (2) and (3) are solved on a square box with periodic boundary conditions using a pseudospectral method with dealiazing according to the 2/3 rule. The initial state is $a_\mathbf{k} = \omega_\mathbf{k} = 0$. Four phases can be distinguished.

(a) Linear stochastic phase. Linearizing Eqs. (2) and (3) $a_\mathbf{k} = a_\mathbf{k}^0 + \tilde{a}_\mathbf{k}$, $\phi_\mathbf{k} = \tilde{\phi}_\mathbf{k}$, $a_\mathbf{k}^0 = \sum_i f_a(t_i)\Delta t$, we can derive the spectra $\tilde{E}_k^M, \tilde{E}_k^V$ in the initial period. Because of the white-noise property of f_a the magnetic energy E^M in Δk increases linearily in time, $E^M(t) = \epsilon t$, $\epsilon = dE^M/dt$. Omitting the straightforward, but somewhat tedious algebra we obtain

$$\tilde{E}_k^V = a_1 (\Delta k)^2 \frac{1}{k_0} \epsilon^2 t^4, \tag{4}$$

$$\tilde{E}_k^M = a_2 (\Delta k)^2 \frac{k^5}{k_0^4} \epsilon^3 t^7, \tag{5}$$

where a_1, a_2 are numerical factors. Hence $\tilde{E}_k^V$ is flat (the same behavior is obtained in the Navier-Stokes case [6]), while $\tilde{E}_k^M \propto k^5$. Although the system is driven only magnetically, the induced spectral kinetic energy is initially much larger than the magnetic one, $\tilde{E}_k^V \gg \tilde{E}_k^M$, but the latter rapidly catches up and reaches the former at $k \simeq k_0$, which initiates the nonlinear phase, where both are tied together, $\tilde{E}_{k_0}^M \simeq \tilde{E}_{k_0}^V$. Rapid growth of $\tilde{E}_k^M, \tilde{E}_k^V$ continues, until the induced spectrum in the dissipation range is high enough to balance the energy input, at which point the total energy saturates, staying constant henceforth except in the asymptotic condensation phase (d).

(b) Nonlinear cascade phase. The mean square potential A grows linearly in time, which drives the inverse cascade process. Figure 1 shows the resulting spectra of A_k, E_k^M, E_k^V. A_k exhibits an almost precise $k^{-7/3}$ law with $C_A = 2.6 \pm 0.2$ using three simulation runs with (a) resolution 512^2 and $\epsilon_A \simeq 2.6 \times 10^{-6}$; (b) 1024^2, $\epsilon_A \simeq 10^{-4}$; (c) 512^2, $\epsilon_A \simeq 6 \times 10^{-4}$. Since Eq. (1) is derived neglecting the Alfvén effect, the present results confirm that this effect is weak in the inverse cascade. The magnetic energy spectrum is close to $k^{-1/3}$, the kinetic one close to $k^{1/3}$. The reduced spectrum $E_k^R = E_k^M - E_k^V$ is positive and scales approximately as $k^{-4/3}$. It is worth noting that the normalized reduced spectrum $E_k^R/E_k \propto k^{-1}$ is steeper than observed in freely decaying turbulence, where $E_k^R/E_k \propto k^{-1/2}$ due to the Alfvén effect as observed in [3] for the direct cascade. Hence in the present case the system tolerates larger differences between E_k^M and E_k^V in the inertial range, which is consistent with the absence of an Alfvén effect.

As the inverse cascade proceeds, coherent magnetic structures increasingly dominate the spatial distribution $a(x,y)$ as illustrated in Fig. 2(a). These structures are generated by current filaments of diameter $\simeq k_0^{-1}$, which locally condense out of the stochastic sea of current density fluctuations. The cascade dynamics is governed by the coalescence of such magnetic eddies. Coalescence is much faster than in decaying MHD turbulence [3], since the high level of small-scale fluctuations induces an anomalous resistivity, allowing fast reconnection. Figure 3 illustrates this effect by comparing the coalescence of two eddies of the state given in Fig. 2(a) with the corresponding two eddy system with the same values of $\eta_4 = \nu_4$ but no small-scale turbulence, $d(t)$ giving the distance between the current filaments. In the latter case the reconnection process starting at $t \approx 46$ is much slower. The turbulent reconnection can be modeled using the results of Refs. [1,9]. Note that because of the attractive forces between parallel currents magnetic eddies coalesce more frequently than vorticity eddies in 2D Navier-Stokes turbulence, the latter primarily circling around each other. We also note, that the quasisingular magnetic structures seen in Fig. 2 are rather different from the rounded magnetic eddies corresponding to smoothly distributed currents seen in the inverse A_k cascade in freely decaying MHD turbulence [3].

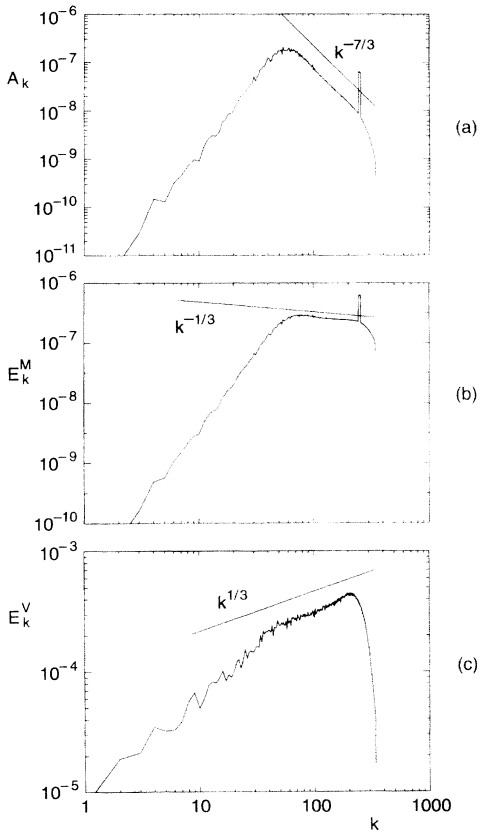

FIG. 1. Spectra of A_k, E_k^M, E_k^V in the cascade phase, obtained from a 1024^2 simulation with pure magnetic driving, $f_\omega = 0$.

As in the case of the inverse energy cascade in 2D Navier-Stokes turbulence [6], the statistics of the veloc-

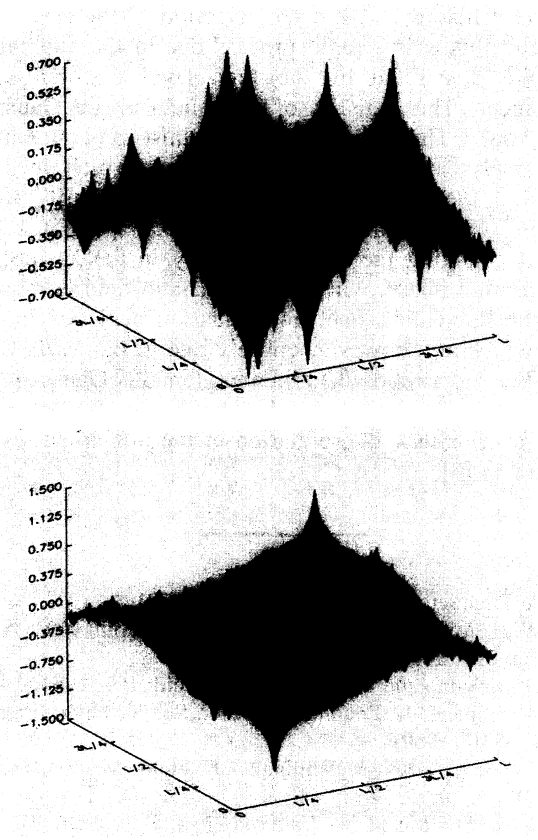

FIG. 2. Distribution of the magnetic potential $a(x, y)$ in the coalescence phase (a), in the condensation phase (b), obtained from a 512^2 simulation.

ity and magnetic field increments δv_l [$= v_x(x + l) - v_x(x)$], δB_l are found to be strictly Gaussian at all scales. This seems in fact to be a general feature of inversely cascading systems. We observe a similar behavior in a shell model of MHD turbulence (even though this model does not reproduce the spectral properties of the fluid system). The statistics also do not depend sensitively on those of the driving forces, remaining almost Gaussian even for constant forces.

(c) Condensation phase. During the inverse cascade process the ground state mode A_1 grows linearly in time as the spectral front propagates to smaller k. Condensation starts when A_1 reaches the spectral level (1). Since the energy flux from k_0 to smaller k is zero, the total energy remaining (statistically) constant also in the condensation phase, the growth of the ground state energy $E_1 = A_1$ results in an energy loss of the higher-k modes $1 < k < k_0$, i.e., an increase of the spectral index ν, $E_k \propto k^{-\nu}$,

$$E_1 + \sum_{k>1} E_k = E_1 + \frac{c}{\nu - 1} = \text{const.} \qquad (6)$$

The spatial distribution of the coherent part of a in this state consists of both the ground state potential $\propto \sin x + \sin y$ and the potential of a pair of antiparallel

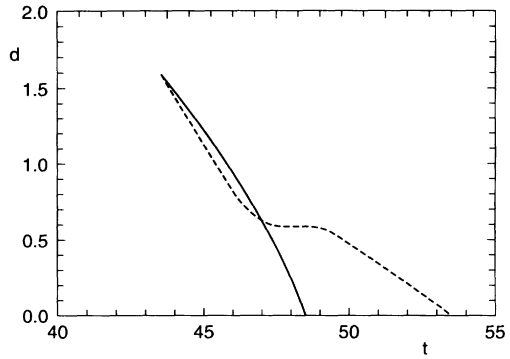

FIG. 3. Distance $d(t)$ between two coalescing magnetic eddies: full simulation (full line), two isolated eddies without small-scale turbulence (dashed line).

line currents [Fig. 2(b)], which has a broad spectrum. Since the energy associated with the current filaments is larger than the contribution of that of the ground state $k = 1$, condensation occurs primarily in x space (condensation of current filaments) rather than in k space. Hence the term Bose condensation used in [6] is misleading. Only in freely decaying MHD turbulence relaxation to the ground state occurs.

The statistics of δB_l and δv_l remain Gaussian also in the condensation phase. No change at any scale is observed when passing from the state in Fig. 2(a) to that of Fig. 2(b). This invalidates the supposition that breaking the self-similarity of the inverse cascade introduces non-Gaussian statistics. Our results seem to be different from the 2D Navier-Stokes case [6], where strong deviations of δv_l from Gaussianity are reported to occur in the condensation phase. This point will be clarified in the following paragraph.

(d) Asymptotic condensation phase. Though the coherent part of the state in Fig. 2(b) contains most of the mean square potential A, its energy contribution is still small compared with the total energy E. This contribution grows linearly in time and after reaching a finite fraction of E, the latter starts to increase, too, invalidating relation (6). In this asymptotic phase, where the coherent quasistatic field generated by the two current filaments dominates over that of the small-scale turbulence, the statistics of δB_l become increasingly non-Gaussian, while those of δv_l remain Gaussian. This seems to contradict the expectation, that the strong large-scale field should couple small-scale magnetic and kinetic fluctuations and therefore their statistics due to the Alfvén effect. To investigate this discrepancy more closely, we generate a much further evolved state simply by multiplication of the current density in the two filaments by some factor $\kappa > 1$ and subsequent relaxation until the statistics have reached a new quasistationary level. Figure 4 shows $F_6 = \langle \delta B_l^6 \rangle / \langle \delta B_l^2 \rangle^3$ for several values of κ. The lower

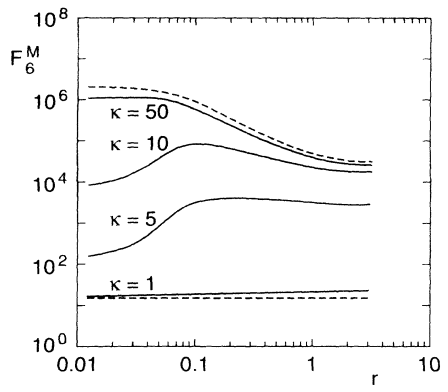

FIG. 4. $F_6 = \langle \delta B_l^6 \rangle / \langle \delta B_l^2 \rangle^3$ in the asymptotic condensation phase.

dashed curve is the Gaussian $F_6 = 15$, while the upper dashed curve gives F_6 for the static contribution of the $\kappa = 50$ state. Hence the non-Gaussian statistics are generated by the quasisingular structure of the *static* field near the filaments of width $\approx k_0^{-1}$, while the superimposed turbulent fluctuations δB_l remain perfectly Gaussian, as found by eliminating the coherent current filaments by choosing $\kappa = 0$. This can be related to a recent result concerning the equilibrium statistics of the MHD fluctuations about a static field [10]. We have also investigated the 2D Navier-Stokes case. Here, too, contrary to the interpretation given in [6], the non-Gaussian statistics in the condensation phase are only due to the quasistationary flows generated by the two antiparallel vorticity filaments, while the superimposed turbulence remains Gaussian.

In conclusion, we have shown that the inverse cascade of A_k in 2D MHD turbulence proceeds by coalescence of current filaments. The reconnection of the associated magnetic flux a is a rapid process due to the anomalous resistivity generated by the high level of small-scale turbulence. The statistics of δB_l and δv_l are Gaussian throughout. This seems to be a robust general feature of inversely cascading turbulent systems, which does not depend on the way of forcing or the self-similarity of the cascade, which is broken in the condensation at $k = 1$ without changing the statistics. Only in the asymptotic condensation phase, when the quasistatic field dominates over the fluctuating one, non-Gaussian statistics in δB_l arise, which are, however, entirely due to the *static* field, while the superimposed turbulence remains Gaussian. A similar behavior arises in the 2D Navier-Stokes case, which gives a new interpretation of the numerical results reported in [6].

[1] A. Pouquet, J. Fluid Mech. **88**, 1 (1978).
[2] W. H. Matthaeus and D. Montgomery, Ann. N.Y. Acad. Sci. **357**, 203 (1980).
[3] D. Biskamp and H. Welter, Phys. Fluids B **1**, 1964 (1989).
[4] H. Politano, A. Pouquet, and P. L. Sulem, Phys. Fluids B **1**, 2330 (1989).
[5] See, e.g., J. C. McWilliams, J. Fluid Mech. **146**, 21 (1984).
[6] L. M. Smith and V. Yakhot, Phys. Rev. Lett. **71**, 352 (1993).
[7] R. H. Kraichnan, Phys. Fluids **8**, 1385 (1965).
[8] M. Hossain, W. H. Matthaeus, and D. Montgomery, J. Plasma Phys. **30**, 479 (1983).
[9] D. Biskamp, Plasma Phys. Controlled Fusion **16**, 311 (1984).
[10] M. B. Ischinko and A. V. Gruzinow (to be published).

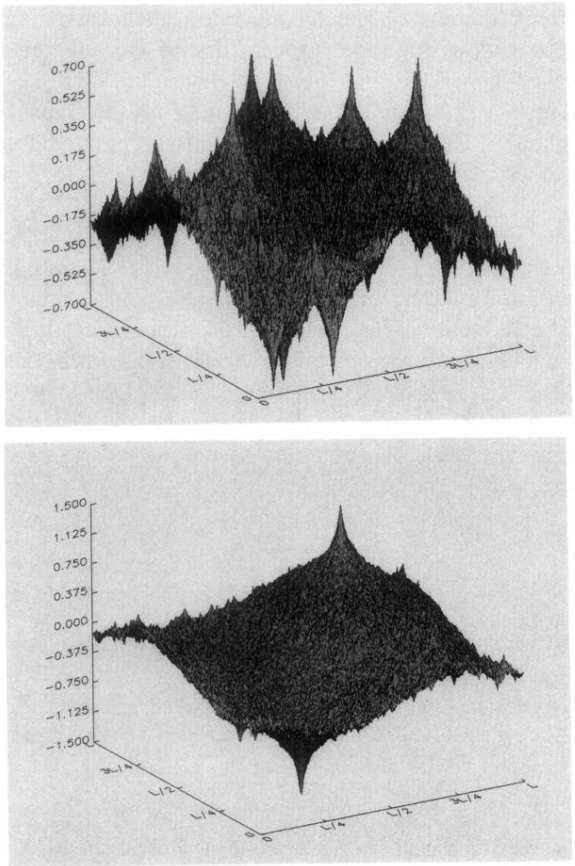

FIG. 2. Distribution of the magnetic potential $a(x, y)$ in the coalescence phase (a), in the condensation phase (b), obtained from a 512^2 simulation.